

# Electron resonant interaction with whistler-mode waves around the Earth's bow shock I: the probabilistic approach

Xiaofei Shi<sup>1</sup>, David S. Tonoian<sup>2,3</sup>, Anton V. Artemyev<sup>1,4</sup>, Xiao-Jia Zhang<sup>2,1</sup>, and Vassilis Angelopoulos<sup>1</sup>

<sup>1</sup>Department of Earth, Planetary, and Space Sciences, University of California, Los Angeles, USA; sxfl698@g.ucla.edu

<sup>2</sup>Department of Physics, University of Texas at Dallas, Richardson, TX, USA; david.tonoian@utdallas.edu

<sup>3</sup>Faculty of Physics, National Research University Higher School of Economics, Moscow, Russia, 105066.

<sup>4</sup>Space Research Institute, RAS, Moscow, Russia

August 14, 2023

## Abstract

Adiabatic heating of solar wind electrons at the Earth's bow shock and its foreshock region produces transversely anisotropic hot electrons that, in turn, generate intense high-frequency whistler-mode waves. These waves are often detected by spacecraft as narrow-band, electromagnetic emissions in the frequency range of  $[0.1, 0.5]$  of the local electron gyrofrequency. Resonant interactions between these waves and electrons may cause electron acceleration and pitch-angle scattering, which can be important for creating the electron population that seeds shock drift acceleration. The high intensity and coherence of the observed whistler-mode waves prohibit the use of quasi-linear theory to describe their interaction with electrons. In this paper, we aim to develop a new theoretical approach to describe this interaction, that incorporates nonlinear resonant interactions, gradients of the background density and magnetic field, and the fine structure of the waveforms that usually consist of short, intense wave-packet trains. This is the first of two accompanying papers. It outlines a probabilistic approach to describe the wave-particle interaction. We demonstrate how the wave-packet size affects electron nonlinear resonance at the bow shock and foreshock regions, and how to evaluate electron distribution dynamics in such a system that is frequented by short, intense whistler-mode wave-packets. In the second paper, this probabilistic approach is merged with a mapping technique, which allows us to model systems containing short and long wave-packets.

## 1 Introduction

The interaction between solar wind electrons and the bow shock results in compressional heating<sup>53,107</sup> and the formation of unstable electron populations which can generate whistler-mode waves<sup>99,100</sup>. A combination of the cross-field thermal anisotropy (due to compression) and a finite heat flux (typical for solar wind electrons<sup>103,93</sup>) provides free energy for whistler-mode waves

in the frequency range of  $\sim [0.1, 0.5]$  of the local electron gyrofrequency<sup>98</sup>. Spacecraft often detect such high-frequency (high compared to whistler-mode magnetosonic waves, also observed in the bow shock<sup>102</sup>), very intense (having amplitudes up to  $\sim 1\%$  of the background magnetic field) whistler-mode waves around the bow shock<sup>105,43,42,81</sup> and in its upstream region<sup>87</sup>. Electron compressional heating upstream (see Ref.<sup>59</sup>) is associated with foreshock transients<sup>96,60</sup>, mesoscale magnetic field perturbations that are formed due to solar wind discontinuity interactions with the bow shock<sup>56,55,76,77</sup>.

In the dense, weakly magnetized plasma around the bow shock (exhibiting a large ratio of plasma frequency to electron gyrofrequency,  $f_{pe}/f_{ce} \geq 100$ ), high-frequency whistler-mode waves may potentially play an important role for 0.1 – 10keV electron scattering<sup>73,72</sup>. Such scattering is an important element of the stochastic shock drift acceleration mechanism<sup>7,67</sup>. Moreover, in the strongly inhomogeneous magnetic field of the bow shock and foreshock transients, intense whistler-mode waves may provide efficient electron acceleration<sup>50,19,86</sup> via nonlinear resonant interactions (see reviews in Refs.<sup>89,4,14</sup> for details). A combination of resonant scattering, shock drift acceleration (with possible contributions from nonlinear resonant interactions), and adiabatic compressional heating has been proposed to explain the formation of relativistic electrons ( $\sim 100\text{keV}$ , i.e.,  $\times 10^4$  higher than the solar wind electron temperature<sup>106</sup>) upstream of the bow shock<sup>104,58</sup>. Explaining electron acceleration in the near-Earth space plasma environment can also be important for astrophysical systems, where shock waves are believed to play a crucial role in electron acceleration<sup>8,26</sup>.

Although the magnetic field configuration of the bow shock and foreshock transients<sup>49,28,102,108</sup>, as well as the statistical properties of high-frequency whistler-mode waves<sup>42,81,87,86</sup> have been well established, the theory of electron resonant interactions with whistler-mode waves in this context is still under development. One complication is that these waves are often sufficiently intense to resonate with electrons nonlinearly (see nonlinearity criterion in Refs.<sup>44,85</sup>). The high wave intensity invalidates the approximations of quasi-linear diffusion theory<sup>44,52</sup> and requires modification of standard models of wave-particle interactions (such modifications have already been made for radiation belt physics, see Refs. of<sup>80,41,40,97,17</sup>). Another complication is that waves propagate in short wave-packets, with a small coherence length (most likely due to the modulation of the waves at their generation region<sup>70,71</sup> and the subsequent wave trapping at the local magnetic field minima formed by compressional ultra-low-frequency perturbations<sup>43,42</sup>). This requires additional modifications of models of nonlinear wave-particle interactions.

There exist two main nonlinear resonance effects: phase trapping and phase bunching<sup>89,4,14</sup>. Both are strongly affected by the wave-packet size (i.e., the wave coherence length): the efficiency of electron acceleration via phase trapping and pitch-angle scattering via phase bunching decrease with decreasing wave-packet size because the particle does not remain in resonance with the wave for a long time<sup>110,91,68,69</sup>. Nonlinear resonant interactions with long wave-packets (those with  $> 20$  wave periods) are non-diffusive and are characterized by large energy/pitch-angle changes for a single resonant interaction<sup>30,78,27</sup>. As the wave-packet shortens, the interaction conforms progressively to a more diffusive treatment, as smaller energy/pitch-angle changes are attained during each resonant interaction with a wave-packet<sup>109,9,6,5,35</sup>. A new modeling approach, going beyond the quasi-linear diffusion and nonlinear resonance theories' assumption of infinitely long wave-packets, is required for electron resonant interactions with whistler-mode waves around the Earth's bow shock.

We have developed such a probabilistic approach model based on the one proposed for wave resonant interactions within electrons bouncing along magnetic field lines in the radiation belts<sup>92,16,61</sup>. The approach assumes multiple, independent resonant interactions described by probability distribution functions (constructed theoretically or derived numerically) of energy and pitch-angle changes during each interaction. Such multiple resonant interactions are possible when particles follow the bounce motion (and periodically attain resonance with the waves) or when they resonate with multi-

ple waves (different wave-packets spatially distributed along particle trajectories). Figure 1 (bottom) depicts the electron dynamics and wave-particle interaction for a foreshock transient (an example is shown on the left) and for a bow shock (an example is shown on the right). In both environments, the background plasma density varies strongly with the background magnetic field (see Fig. 1(a,d) and (h,k)), and the  $f_{pe}/f_{ce}$  ratio is large ( $\approx 100$ ) and almost constant. The whistler-mode wave characteristics are also quite similar in these two environments: waves propagate in the form of intense ( $\sim 1\%$  of background magnetic field), short wave-packets (see Fig. 1(g,n)). This allows us to apply our model to both systems, with equal efficacy. For the bow shock region, we are interested in reflected electrons, which can be scattered by whistler-mode waves upstream and turned back to the shock. These electrons should resonate with waves that are generated upstream and propagating downstream. For the foreshock transients, electrons may be trapped between the shock of the foreshock transient and the bow shock. In that case, the electrons bounce back and forth, undergoing multiple resonant interactions with waves generated within the core of the foreshock transients.

This is the first of two accompanying papers. In this paper, we describe the basic properties of electron resonant interactions with whistler-mode waves and develop a probabilistic approach, which enables tracing the long-term evolution of electron distribution functions. This approach assumes that waves are sufficiently incoherent (wave-packets are short) to reduce the efficiency of nonlinear resonant interactions and hence lead to diffusive particle scatterings. Such a diffusion by intense wave-packets is quite different from the quasi-linear diffusion<sup>88,33,35</sup>. In the second paper, we describe how this probabilistic approach can be merged with a mapping technique<sup>25,46,47,15</sup> to model electron dynamics in systems with a significant effect from nonlinear resonance with long wave-packets.

The rest of the paper includes the following sections: descriptions of the basic equations for wave-particle resonant interactions (Sect. 2), descriptions of the probability distribution of energy and pitch-angle changes (Sect. 3), a numerical verification of the probabilistic approach (Sect. 4), and discussion of the results (Sect. 5). In Sections 2 and 3, we examine the effect of wave-packet size on nonlinear resonance and determine the parametric range of diffusive electron scattering by intense, short wave-packets. Most examples and conclusions are valid for electron dynamics in both bow shock and foreshock transients.

## 2 Basic equations

We use the Hamiltonian model for the nonrelativistic electron (mass  $m_e$ , charge  $-e$ ) dynamics<sup>19</sup>

$$H = \frac{p_{\parallel}^2}{2m_e} + \mu\Omega_0(s) - e\Phi(s) \quad (1)$$

where  $(s, p_{\parallel})$  are conjugate field-aligned coordinates and momentum, the electron cyclotron frequency  $\Omega_0(s) = eB_0(s)/m_e c$  is determined by the ambient magnetic field profile,  $B_0(s)$ , and  $\Phi(s)$  is the electrostatic potential due to decoupling of ion and electron motions around magnetic field gradients<sup>38,83,36</sup>. This model omits the effect of electron heating due to interaction with shock waves, i.e., the Hamiltonian equation is written in the bow shock (or foreshock transient) reference frame, but there is no projection of the shock speed on the field-aligned direction,  $v_D$ . The effect of this shock motion can be added as  $s \rightarrow s + v_D t$  (see Refs.<sup>53,107</sup>), which does not influence the wave-particle resonant interaction, because  $v_D \leq 1000\text{km/s}$  (see Ref.<sup>107</sup>) is smaller than the typical resonant electron velocity  $\geq 5000\text{km/s}$  (see Refs.<sup>86,19</sup>).

To describe the resonant interaction of electrons and field-aligned whistler-mode waves, we add the term  $U_w \cos(\phi + \psi)$  to the Hamiltonian (1), see Refs.<sup>89,4,20</sup>. The wave phase  $\phi$  is determined

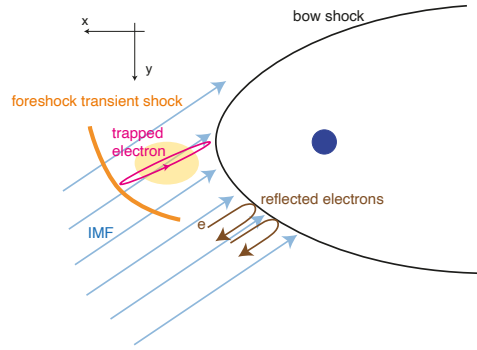
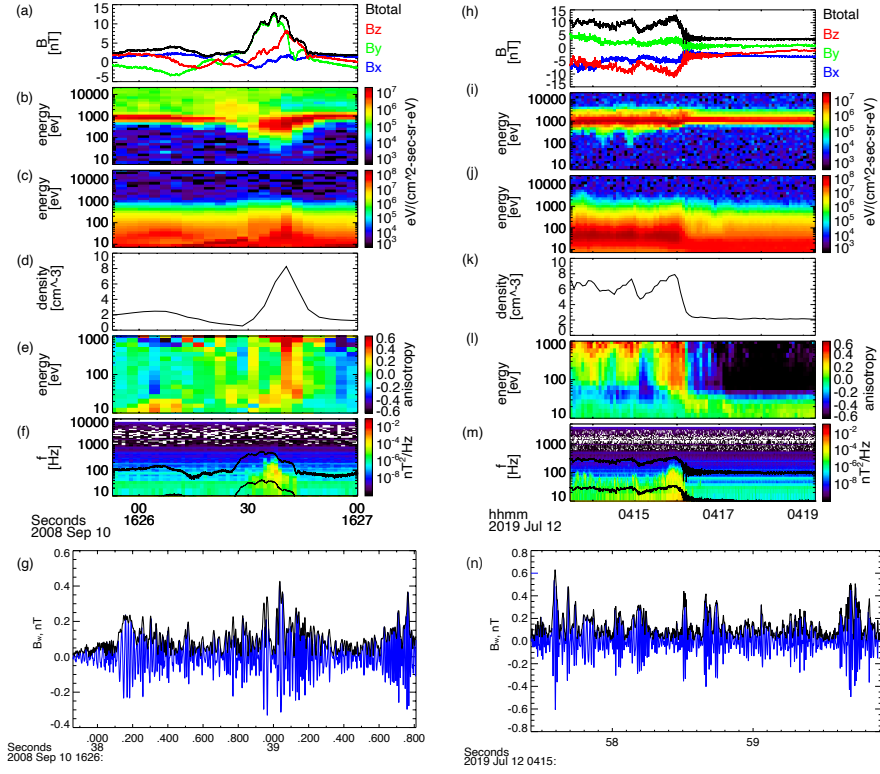


Figure 1: Observations of a foreshock transient (left) and the distant bow shock (right) by the THEMIS spacecraft<sup>10,11</sup>. Fluxgate magnetometer<sup>23</sup> measurements of magnetic fields show a strong peak in the magnetic field magnitude at the foreshock transient (a) and a step-like increase in the magnetic field magnitude at the bow shock (h). Measurements by the electrostatic analyzer<sup>64</sup> show the thermalization of solar wind ion flows (b, i); an increase in the electron temperature (an increase of electron fluxes  $f$  above 1 keV) within the foreshock transient (c) and across the bow shock (j); the formation of a transversely anisotropic electron population at  $> 100\text{eV}$  with  $(f_{\perp} - f_{\parallel}) / (f_{\perp} + f_{\parallel}) > 1$ , where  $f_{\perp}$ ,  $f_{\parallel}$  are electron fluxes averaged over pitch-angle ranges of  $[0, 30^{\circ}]$  and  $[75^{\circ}, 105^{\circ}]$  (e,l); and density increase in correlation with the magnetic field magnitude increase (d,k). Measurements by the search coil magnetometer<sup>51,29</sup> show electromagnetic wave activities within the whistler-mode frequency range (f,m) and examples of typical whistler-mode wave-packets (g,n). Black lines in (f,m) are electron cyclotron frequency and 1/10 of this frequency. Black and blue lines in (f,m) are wave magnetic field magnitude and one of the two transverse magnetic field components. The bottom panel depicts the electron dynamics (brown: reflection; purple: trapping) and wave-particle resonant interactions (in a yellow-highlighted interaction region) at the bow shock (black) and within the foreshock transient (demarcated by the bow shock and the shock upstream of it in orange).

by the wave number  $k(s) = \partial\phi/\partial s$  and the wave frequency  $\omega = -\partial\phi/\partial t$ , whereas  $k = (\Omega_{pe}/c) \cdot (\Omega_0/\omega - 1)^{-1/2}$  is given by the cold plasma dispersion relation<sup>90</sup>. The electron gyrophase  $\psi$  is conjugate to the magnetic moment  $\mu = E \sin^2 \alpha / \Omega_0(s)$ , where  $E$  is the electron energy and  $\alpha$  is the electron pitch-angle. The effective wave energy is  $U_w = \sqrt{2\mu\Omega_0/m_e c^2} e B_w / k$ , where  $B_w$  is the wave magnetic field amplitude<sup>1,97</sup>. The system under consideration contains two smallness parameters,  $\max B_w / \min B_0 \ll 1$  and  $1 / \min kL \sim \max B_w / \min B_0 \ll 1$ , where  $L$  is the spatial scale of the ambient magnetic field variation,  $\Omega_0 = \Omega_0(s/L)$ . The first parameter determines whether the wave term  $\sim U_w$  is a small perturbation in the Hamiltonian  $H$ . The second determines whether the wave phase and gyrophase change much faster than the particle field-aligned coordinate  $s$  and momentum  $p_{\parallel}$ . The resonance condition for this system is  $\dot{\phi} + \dot{\psi} = 0$ :

$$k(s) \frac{\partial H}{\partial p_{\parallel}} - \omega + \frac{\partial H}{\partial \mu} = k(s) \frac{p_{\parallel}}{m_e} - \omega + \Omega_0(s) = 0$$

We build two models for two systems: Earth's bow shock and foreshock transients. For the bow shock, the minimum of the background magnetic field is far upstream,  $s \rightarrow -\infty$ , and the magnetic field is modeled to increase as  $\Omega_0 = \Omega_{\min} \cdot (1 + 3b(s))$  and  $b(s) = (1/2) \cdot (1 + \tanh(s/L))$ . The spatial scale  $L$  is about 1000km, i.e.,  $1 / \min kL \approx c/L \min \Omega_{pe} \sim 10^4$ . This system also has a cross-shock electrostatic potential  $\Phi(s) = \Phi_0 b(s)$ , and plasma frequency  $\Omega_{pe} / \Omega_{pe, \min} = 100 \cdot \sqrt{\Omega_0(s) / \Omega_{\min}}$ . We consider electrons that move toward the shock, then are reflected by the shock, and resonate with whistler-mode waves propagating toward the shock in the upstream region.

The foreshock transient model is characterized by a local magnetic field minimum  $\Omega_0 = \Omega_{\min} \cdot \sqrt{1 + (s/L)^2}$ , and we set  $\Phi = 0$ . For foreshock transients, the plasma frequency  $\Omega_{pe} = 100 \cdot \Omega_0(s)$  (see observations in Ref.<sup>86</sup>). The spatial scale  $L$  is also about 1000km. We consider waves that are generated in the core region (minimum magnetic field) and propagating to both sides. As a result, electrons bouncing within the *magnetic bottle* forming between the bow shock and the foreshock transient shock can resonate with such waves twice per bounce period.

Figure 2 shows examples of electron trajectories from the numerical integration of the Hamiltonian equations of motion for two systems with different parameters. There are two main effects of nonlinear resonant interactions: phase bunching characterized by energy decrease and phase trapping characterized by large energy increase (see Refs.<sup>45,94,2,79</sup>). We aim to describe electron distribution dynamics driven by multiple nonlinear resonant interactions.

### 3 Probability distribution function of $\Delta E$

To characterize wave-particle resonant interactions, we will use the probability distribution  $\mathcal{P}(\Delta E)$  of energy change for a single resonant interaction. For fixed system parameters, this distribution will depend on the initial electron energy  $E$  and pitch-angle  $\alpha_0$ . The pitch-angle can be substituted by the initial electron magnetic moment  $\mu_0 = E \sin^2 \alpha_0 / \Omega_{\min}$  (we set initial conditions at the magnetic field minimum). Equation (1) after adding the wave term,  $U_w \cos(\phi + \psi)$ , has one integral of motion:  $E - \omega\mu = h = \text{const}$  (see, e.g., Ref.<sup>89</sup>). This is a constant because there are no electric fields in the reference frame moving with the wave ( $t \rightarrow t + \omega t$ ), and the particle energy  $\sim h$  in this reference frame is conserved. Therefore, we can use the probability distribution function  $\mathcal{P}(\Delta E, E)$  defined in the  $(\Delta E, E)$  space for fixed  $h$ . For waves with infinitely long wave-packets  $\sim \cos(\phi + \psi)$ , such probability distribution functions can be derived analytically<sup>97,22</sup>. In reality, however, waves propagate in the form of wave-packets (see Fig. 1 and Refs.<sup>43,42,86</sup>), where  $\mathcal{P}$  can only be determined from numerical simulations<sup>80,41,21</sup>. We introduce the wave field modulation,  $\cos(\phi + \psi) \rightarrow f(\phi) \cos(\phi + \psi)$ , and

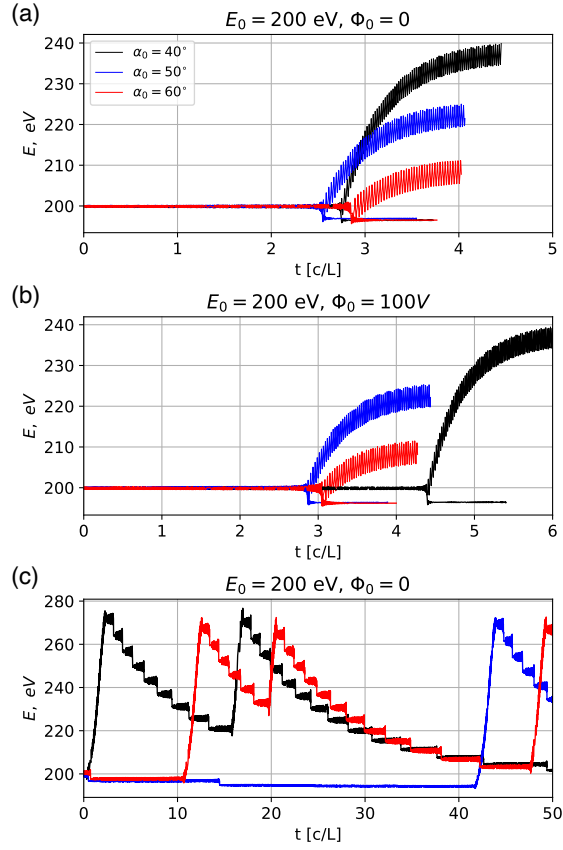


Figure 2: Examples of electron energy evolution due to the interactions with the prescribed wave field (energy versus time): for the bow shock model with  $\Phi_0 = 0$  (a), for the bow shock with  $\Phi_0 = 100$  V (b), and for the foreshock transient (c). Each panel shows three trajectories with the same initial energy 200 eV and three different initial pitch-angles.

numerically evaluate  $\mathcal{P}$  for different modulation characteristics. Function  $f(\phi)$  describes the wave-packet train, and we use a simple form  $f(\phi) = \exp(-5 \cdot \cos^2(\phi/2\pi\beta))$  with  $\beta$  denoting the wave-packet size<sup>95</sup>. An additional model parameter is the wave phase coherence number measured by the number of contiguous coherent wave packets,  $N_c$ . This parameter describes how many wave packets within the train have the same initial  $\phi$ , i.e., maintain phase coherence from one packet to the next one. The limit  $N_c \rightarrow \infty$  corresponds to the situation when all wave packets are generated in the same source region by the same particle population, so there is no variation (destruction) of the wave phase among wave packets (in this case electrons may be trapped into the next wave packet after escaping from the previous one, and such multi-trapping would result in effective electron acceleration, similar to infinitely long wave-packets<sup>39</sup>). However, different wave-packets are often generated in different source regions and their phases are not coherent across the entire packet train<sup>109</sup>. This effect can be modeled by a finite  $N_c$ , which will reduce the efficiency of the phase trapping and acceleration.

### 3.1 Long wave-packets

During a simulation of many electrons interacting with wave-packets of a given frequency,  $N_c$  and  $\beta$ , the value of  $h$  remains fixed throughout the resonant interaction, and the resultant energy change can be obtained from a probability distribution of  $\Delta E$  for the fixed  $h$ . We can therefore use a  $\Delta E$  lookup table for the given fixed  $h$  of an electron of an initial pitch angle and associated resonance energy. The full range of initial equatorial pitch angles ( $30^\circ$  to approximately  $80^\circ$  at the minimum of the magnetic field magnitude) will map to a range of resonance energies around 220–280eV and result in a 2-D probability distribution quantifying the results of the interaction. Figure 3 shows probability distributions  $\mathcal{P}(\Delta E, E)$  for the fixed  $h$  and long wave-packets ( $\beta = 100$ ,  $N_c \rightarrow \infty$ ). There is a clear dependence of  $\Delta E$ -distribution on initial energy,  $E_0$ . For small  $E_0$ , the distribution of energy changes shows two distinct populations: a small number of electrons with very large  $\Delta E > 0$  are electrons accelerated via phase trapping, whereas the main electron population has small  $\Delta E < 0$  due to phase bunching. With the increase of the initial energy,  $E_0$ , the trapping acceleration becomes less effective and the trapped population moves closer to  $\Delta E \sim 0$ . This is caused by the value of the resonance energy: for fixed  $h$ , smaller  $E_0$  means smaller  $\alpha_0$  and larger  $s$  for the resonant interactions where electrons will be trapped. As all trapped electrons escape from the resonance at  $s \sim 0$ , which corresponds to minimum  $B_0$ , the duration of electron trapping increases with larger values of  $s$  (see Refs.<sup>89,80,20</sup> for a discussion of trapped electron acceleration in an inhomogeneous magnetic field). This leads to longer trapping times and more significant acceleration. Therefore, for long, coherent wave-packets (large  $\beta$ , large  $N_c$ ) the probability distribution of energy changes,  $\mathcal{P}(\Delta E, E)$ , depends on two parameters ( $E, h$ ). To describe electron dynamics, we need to determine the probability distribution in 3D space of  $(\Delta E, E_0, h)$ . This can be done analytically because  $\Delta E$  can be determined from analysis of the Hamiltonian equation (1) with the wave term included<sup>97,15</sup>, and we will provide such a solution in the second paper.

However, as we shall see in the next subsection, a further simplification in the statistical description of the resonant interactions is possible when the wave-packets are short. In that case, the dependence on  $E_0$  is weak, and the interactions can be well-described as a 1-D probability distribution over a narrower energy range. This simplification with the help of a cumulative probability function leads to the probabilistic approach which we will discuss in the next section.

### 3.2 Short wave-packets

Although it is possible to obtain an analytical model for resonant interactions between long wave packets and electrons, such long wave packets are rarely observed. In contrast, the majority of

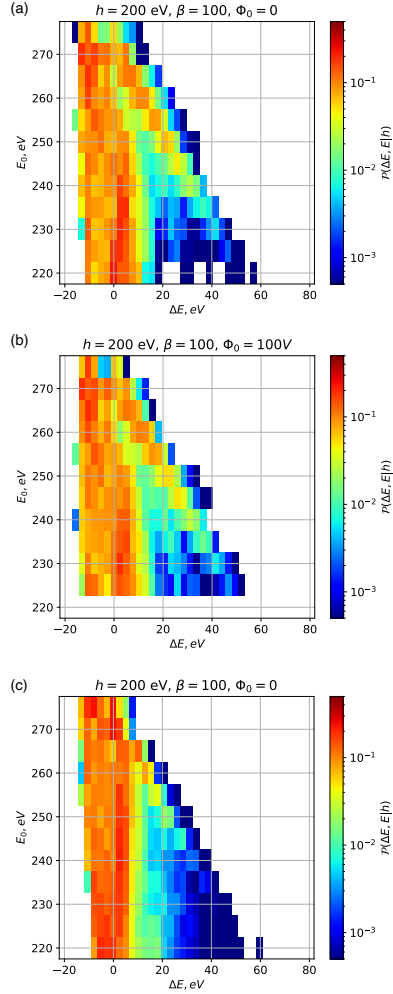


Figure 3: Examples of  $\mathcal{P}(\Delta E, E_0)$  distributions for the bow shock model with  $\Phi_0 = 0$  (a), for the bow shock model with  $\Phi_0 = 100V$  (b), for the foreshock model (c); in all cases,  $N_c \rightarrow \infty$  and  $\beta = 100$ . The main difference between (a) and (b) is that for  $\Phi_0 = 100V$  many electrons with resonant energies  $\leq 225$ eV cross the bow shock and do not resonate with waves in the upstream region.



observations are of short wave packets (see Fig. 1 and Ref.<sup>86</sup>). For these, the efficiency of trapping acceleration varies from one interaction to another, and the role of initial conditions becomes much less important. To illustrate this, we calculate the  $\mathcal{P}(\Delta E, E)$  distribution for fixed  $h$  and small  $\beta$ ,  $N_c$ . Figure 4 shows that in the short wave-packet limit, the  $\Delta E$  -distribution is mainly distributed within 20eV of  $\Delta E = 0$ , with no significant probability of large positive values of  $\Delta E$ . This implies that the energy gained by trapped electrons decreases (due to the shorter time that electrons spend in the trapping acceleration, see, e.g., Refs<sup>91,110,68</sup>), while the number of trapped electrons increases (due to large gradient of the wave amplitude at the edge of wave-packet, see, e.g., Ref.<sup>27,21,9</sup> and the second paper). Such a  $\Delta E$ -distribution can be characterized by two parameters,  $\langle \Delta E \rangle$  and  $\langle (\Delta E)^2 \rangle$ , i.e., the wave-particle interaction is diffusive. However, this diffusion,  $\langle (\Delta E)^2 \rangle \propto B_w^\kappa$  with  $\kappa \sim 1$ , caused by almost monochromatic intense waves is quite different from the quasi-linear diffusion with  $\langle (\Delta E)^2 \rangle \propto B_w^2$  (see the theoretical model for  $\langle (\Delta E)^2 \rangle$  in Ref.<sup>33</sup>). In addition to the symmetric distribution of  $\Delta E$ , short wave-packets also have another important effect. As depicted in Figure 4,  $\mathcal{P}(\Delta E, E)$  now exhibits weak dependence on  $E$  for fixed  $h$ . Therefore, instead of a 2D  $\mathcal{P}(\Delta E, E)$ , we can use a 1D distribution,  $\bar{\mathcal{P}}(\Delta E) = \langle \mathcal{P}(\Delta E, E) \rangle_E$ , to describe the interaction around the specific resonance energy  $E$ , for a fixed  $h$ .

## 4 Verification of the probabilistic approach

Figure 4 shows that for systems with short wave packets, we may use a 1D  $\bar{\mathcal{P}}(\Delta E)$  distribution. This distribution is equivalent to the cumulative probability distribution  $\mathcal{C}(\Delta E) = \int_{-\infty}^{\Delta E} \bar{\mathcal{P}}(x) dx$ , which can be used for tracing the electron resonant energy change: given a random number  $\xi_n \in [0, 1]$ , one can find the corresponding  $\Delta E$  using  $\mathcal{C}(\Delta E) = \xi_n$  distribution. The energy change for each interaction is  $E_{n+1} = E_n + \Delta E(\xi_n)$ , where  $n$  is the iteration number (number of resonant interactions). Figure 5(a) shows  $\mathcal{C}(\Delta E)$  for  $\bar{\mathcal{P}}(\Delta E) = \langle \mathcal{P}(\Delta E, E) \rangle_E$  from Fig. 4(c), whereas Fig. 5(b) shows several trajectories  $E_n$  evaluated with this probabilistic approach. For comparison, we also plot  $E_n$  trajectories (Fig. 5(c)) obtained from the numerical integration of original Hamiltonian equations with the system parameters in the caption of Fig. 4. Figures 5(b,c) demonstrate that this  $\mathcal{C}$ -based probabilistic approach and the numerical integration approach provide very similar patterns of electron energy dynamics.

We use the foreshock transient model because for this situation we may reproduce multiple resonant interactions with the wave having a fixed frequency (also fixed  $h$ ) as electrons bounce between mirror points. Resonant wave-particle interactions alter electron pitch-angles and thus may move their mirror points sufficiently far from  $s = 0$  to cause electron losses. We set the magnetic field trapping ratio as  $\max B / \min B = 10$ , in agreement with statistical observations of magnetic field variations in the foreshock transients<sup>86</sup>. Thus, electrons with pitch-angles (referenced at magnetic field minimum) below  $\sim 18^\circ$  escape from the foreshock transient. The energy range of resonant interactions for fixed  $h$  (e.g., as shown for  $\mathcal{P}(\Delta E, E_0)$  in Figs. 4, 5) includes such small pitch-angles (corresponding to  $h = E - \omega\mu \approx E$ ). It is important to note two significant points regarding small pitch-angle/field-aligned electrons. First, field-aligned electrons can escape from the foreshock transients and cross the bow shock without reflection. Second, field-aligned electrons resonate with waves in a specific regime that excludes pitch-angle/energy reduction<sup>62</sup>. The nonlinear resonant interactions in this regime are characterized by  $\sim 100\%$  phase trapping with pitch-angle/energy increase (see results of numerical simulations in Ref.<sup>48,34</sup> and theoretical models in Refs.<sup>3,13</sup>). These two effects complicate the modeling of field-aligned electron dynamics. To resolve this issue, we employ the following procedure: electrons with pitch-angles below  $18^\circ$  are allowed to escape from the foreshock transient; however, to keep the number of electrons unchanged

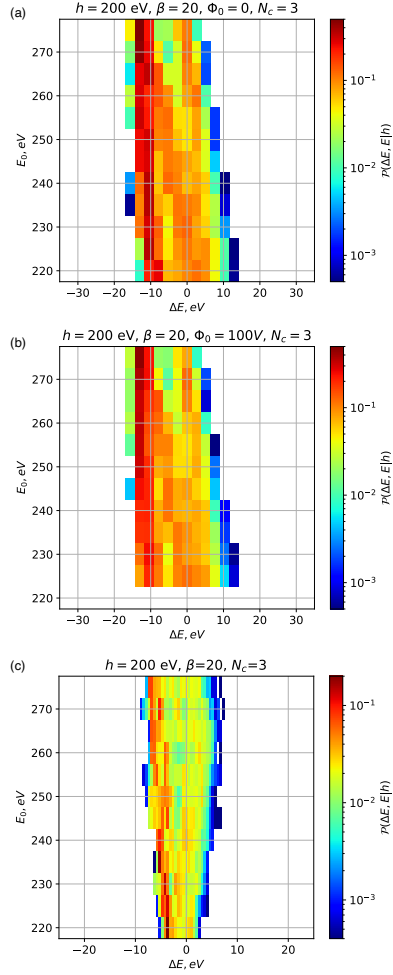


Figure 4: Examples of  $\mathcal{P}(\Delta E, E)$  distributions for the bow shock model with  $\Phi_0 = 0$  (a), for the bow shock model with  $\Phi_0 = 100V$  (b), for the foreshock model (c);  $N_c = 10$  and  $\beta = 20$ . The main difference between (a) and (b) is that for  $\Phi_0 = 100V$  a considerable number of electrons with resonant energies  $\leq 225eV$  cross the bow shock and do not resonate with waves in the upstream region.

we re-introduce the same number of electrons into the system with their initial pitch-angles and energies. The replacement electrons can be thought of as solar wind electrons that become trapped within the foreshock transient.

To further verify the probabilistic approach, we use the  $\mathcal{C}$  function to evaluate energies of  $10^5$  trajectories for 20 resonant interactions. We use the initial distribution function  $F(E) \sim \exp(-E/50\text{eV})$  to set the initial phase space density  $F(E)$  and then trace its evolution in energy. Note that this is a 1D distribution for a fixed  $h$ ; to trace the dynamics of a 2D (energy, pitch-angle) distribution, numerous  $h$  should be used<sup>97</sup>. To compare and validate the results obtained from the probabilistic approach, we use  $10^4$  numerically integrated electron trajectories with the same initial distribution  $F(E)$ . Figure 6 shows  $F_m(E)$  for the probabilistic approach and  $F_t(E)$  for test particle simulations with different  $n$ . Note that although we use iteration numbers instead of time, the same approach can be used for the time iteration,  $t_{n+1} = t_n + \tau(E_n)/2$ , with  $\tau(E_n)$  being the bounce period of electrons, i.e.,  $\tau(E_n)/2$  is the time between two resonant interactions. The scattering caused by short wave-packets mostly results in an energy decrease (which also means the pitch-angle decrease), and  $F_t(E)$ ,  $F_m(E)$  grow at smaller energies. The electron distribution obtained by test particle simulations evolves very similar to that obtained from the probability approach, i.e., the probability approach works well.

## 5 Discussion

This is the first of two papers devoted to developing a theoretical approach for modeling solar wind electron scattering and acceleration by high-frequency whistler-mode waves around the Earth's bow shock. We examine the resonance effects of the most widespread wave population which consists of short, intense wave-packets. Although an individual resonant interaction with a short wave packet includes nonlinear effects such as phase trapping and bunching<sup>79,89,4</sup>, the magnitude of energy/pitch-angle change due to trapping and bunching are comparable, and the particle dynamics resembles diffusion<sup>18</sup>. The corresponding diffusion coefficients, however, differ from the coefficients predicted by the quasi-linear diffusion theory<sup>33</sup>. Thus, instead of using linear theory and the Fokker-Plank equation<sup>82,63</sup>, we use the probabilistic approach. This approach repeats the general stochastic differential equation method for wave-particle resonant interactions<sup>92</sup>, but does not make any assumptions about the diffusive nature of the interactions<sup>21,61</sup>.

Interactions between the solar wind electrons and the bow shock/foreshock transients include multiple effects operating on different temporal and spatial scales: electron acceleration by ion-scale electrostatic fields that form due to decoupling of ion and electron motions around strong magnetic field gradients<sup>53,107,83</sup>; electron demagnetization and scattering by small-scale, intense electrostatic fields<sup>24,84,37</sup>; electron trapping and adiabatic pumping by ultra-low frequency compressional fluctuations of the magnetic field<sup>54</sup>; electron spatial mixing by turbulent electromagnetic fields<sup>65,66</sup>, etc. The description of most of these effects requires temporal and spatial resolution on the scales of ion kinetics, which is reachable in modern hybrid simulations<sup>77,75,101,57,74</sup>. The test particle approach for electron tracing in electromagnetic fields from hybrid simulations can describe all details of hot electron dynamics<sup>58</sup> except wave-particle interaction effects, which are principally important for electron scattering and shock drift acceleration<sup>8</sup>. Thus, in the future we propose to incorporate resonant wave-particle interaction effects in test particle simulations by employing the probabilistic approach (such an approach has been extensively used at the Earth's inner magnetosphere<sup>32,31</sup>, but has never been considered for the bow shock).

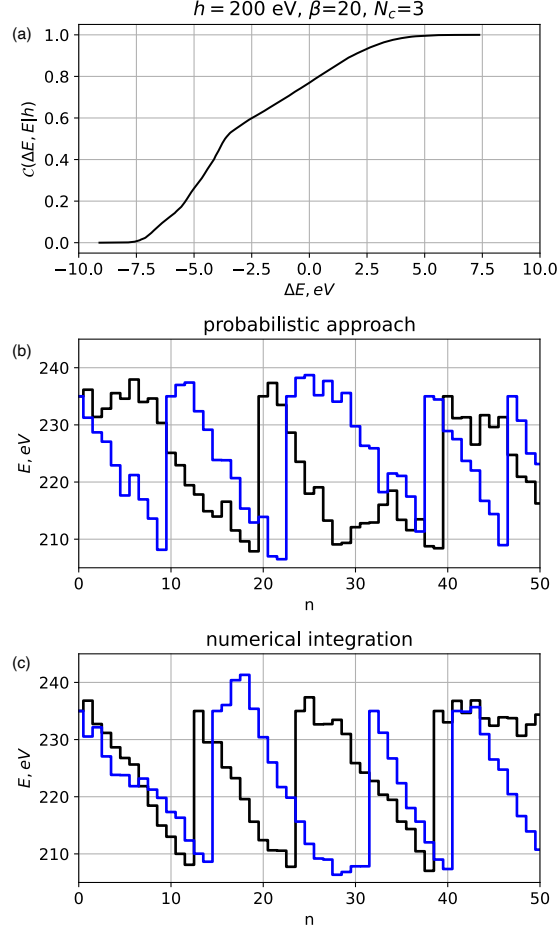


Figure 5: Panel (a) shows the cumulative probability distribution function  $\mathcal{C}(\Delta E)$  for  $\tilde{\mathcal{P}}(\Delta E)$  from Fig. 4(c). Panels (b,c) shows electron energy as a function of the number of resonant interactions  $n$  (two interactions per bounce period) for several electron trajectories evaluated with the probabilistic approach (b) and with numerical integration of original Hamiltonian equations (c). The system configuration and parameters are the same as in Fig. 4(c).

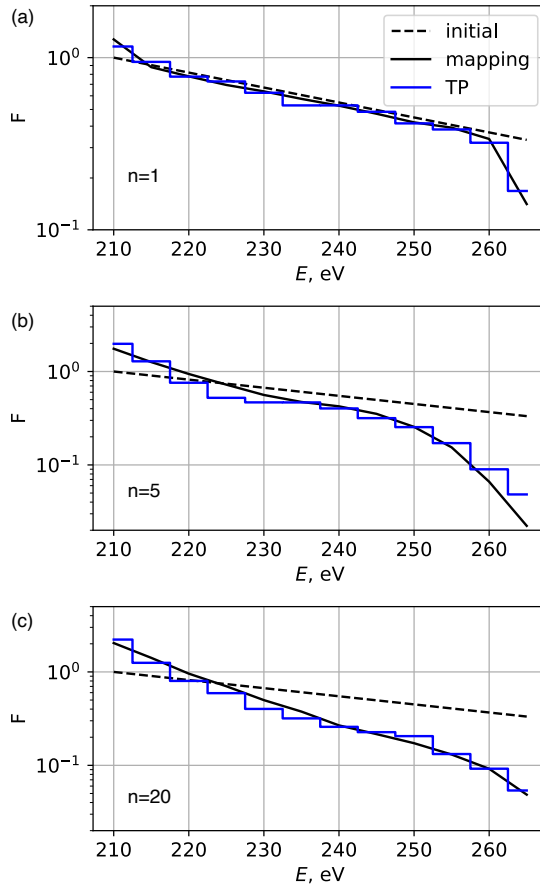


Figure 6: Evolution of electron distribution function evaluated by numerical integration of Hamiltonian equations (1) and by the probabilistic approach using the cumulative distribution  $\mathcal{C}$  of Fig. 5(a). Three panels show results for  $n = 1$ (a),  $n = 5$ (b), and  $n = 20$ (c); the dashed curve in each panel shows the normalized initial distribution,  $F(E) \sim \exp(-E/50\text{eV})$ ; blue curves show results of test particle simulations, black curves show results of the probabilistic approach.

## 6 Conclusions

In this study, we modeled resonant interactions between solar wind electrons and intense short wave-packets of whistler-mode waves. For two magnetic field configurations, corresponding to the foreshock transient and Earth’s bow shock, we demonstrate that:

- The nonlinear resonant effect, phase trapping, is modified for short wave packets: the probability of trapping becomes larger, whereas energy change due to single trapping becomes smaller. The phase bunching is barely affected by the wave-packet size. Thus, the  $\Delta E$ -distribution of electron energy change due to a single resonant interaction can be averaged over initial energies to derive the cumulative probability distribution  $\mathcal{C}(\Delta E) = \int_{-\infty}^{\Delta E} \bar{\mathcal{P}}(x) dx$  for modeling the electron energy evolution  $E_{n+1} = E_n + \Delta E(\xi_n)$  with  $\mathcal{C}(\Delta E) = \xi_n$ .
- We have proposed and verified the probabilistic approach based on  $\bar{\mathcal{P}}(\Delta E)$  probability distributions to describe electron energy variations.
- This probabilistic approach can be used to model the long-term dynamics of electron distributions in a system with multiple nonlinear resonant interactions with short wave-packets.

In the second paper, we will further generalize this approach for systems with a finite probability of electron resonant interactions with long wave-packets.

## Acknowledgments

X.S., A.V.A., X.-J.Z., and V.A. acknowledge THEMIS contract NAS5-02099, NASA grants 80NSSC22K1634, 80NSSC21K0581 (spacecraft data analysis and numerical simulations). A.V.A. and D.S.T. also acknowledge Russian Science Foundation through grant No. 19-12-00313 (theoretical models).

## Data Availability

This is a theoretical study, and all figures are plotted using numerical solutions of equations in the paper. The data used for figures and findings in this study are available from the corresponding author upon reasonable request. Spacecraft data for the first figure are openly available in THEMIS data repository <https://themis.igpp.ucla.edu/>. Data access and processing were done using SPEDAS V4.1<sup>12</sup>.

## References

- [1] Albert, J.M., 1993. Cyclotron resonance in an inhomogeneous magnetic field. *Physics of Fluids B* 5, 2744–2750. [10.1063/1.860715](https://doi.org/10.1063/1.860715).
- [2] Albert, J.M., 2000. Gyroresonant interactions of radiation belt particles with a monochromatic electromagnetic wave. *J. Geophys. Res.* 105, 21191. [10.1029/2000JA000008](https://doi.org/10.1029/2000JA000008).
- [3] Albert, J.M., Artemyev, A.V., Li, W., Gan, L., Ma, Q., 2021. Models of resonant wave-particle interactions. *Journal of Geophysical Research: Space Physics* 126, e2021JA029216. [10.1029/2021JA029216](https://doi.org/10.1029/2021JA029216).

- [4] Albert, J.M., Tao, X., Bortnik, J., 2013. Aspects of Nonlinear Wave-Particle Interactions, in: Summers, D., Mann, I.U., Baker, D.N., Schulz, M. (Eds.), Dynamics of the Earth's Radiation Belts and Inner Magnetosphere. 10.1029/2012GM001324.
- [5] Allanson, O., Watt, C.E.J., Allison, H.J., Ratcliffe, H., 2021. Electron Diffusion and Advection During Nonlinear Interactions With Whistler Mode Waves. *Journal of Geophysical Research (Space Physics)* 126, e28793. 10.1029/2020JA028793.
- [6] Allanson, O., Watt, C.E.J., Ratcliffe, H., Allison, H.J., Meredith, N.P., Bentley, S.N., Ross, J.P.J., Glauert, S.A., 2020. Particle-in-Cell Experiments Examine Electron Diffusion by Whistler-Mode Waves: 2. Quasi-Linear and Nonlinear Dynamics. *Journal of Geophysical Research (Space Physics)* 125, e27949. 10.1029/2020JA027949.
- [7] Amano, T., Katou, T., Kitamura, N., Oka, M., Matsumoto, Y., Hoshino, M., Saito, Y., Yokota, S., Giles, B.L., Paterson, W.R., Russell, C.T., Le Contel, O., Ergun, R.E., Lindqvist, P.A., Turner, D.L., Fennell, J.F., Blake, J.B., 2020. Observational Evidence for Stochastic Shock Drift Acceleration of Electrons at the Earth's Bow Shock. *Phys. Rev. Lett.* 124, 065101. 10.1103/PhysRevLett.124.065101, arXiv:2002.06787.
- [8] Amano, T., Matsumoto, Y., Bohdan, A., Kobzar, O., Matsukiyo, S., Oka, M., Niemiec, J., Pohl, M., Hoshino, M., 2022. Nonthermal electron acceleration at collisionless quasi-perpendicular shocks. *Reviews of Modern Plasma Physics* 6, 29. 10.1007/s41614-022-00093-1, arXiv:2209.03521.
- [9] An, Z., Wu, Y., Tao, X., 2022. Electron Dynamics in a Chorus Wave Field Generated From Particle-In-Cell Simulations. *Geophys. Res. Lett.* 49, e97778. 10.1029/2022GL097778.
- [10] Angelopoulos, V., 2008. The THEMIS Mission. *Space Sci. Rev.* 141, 5-34. 10.1007/s11214-008-9336-1.
- [11] Angelopoulos, V., 2011. The ARTEMIS Mission. *Space Sci. Rev.* 165, 3-25. 10.1007/s11214-010-9687-2.
- [12] Angelopoulos, V., Cruce, P., Drozdov, A., Grimes, E.W., Hatzigeorgiu, N., King, D.A., Larson, D., Lewis, J.W., McTiernan, J.M., Roberts, D.A., Russell, C.L., Hori, T., Kasahara, Y., Kumamoto, A., Matsuoka, A., Miyashita, Y., Miyoshi, Y., Shinohara, I., Teramoto, M., Faden, J.B., Halford, A.J., McCarthy, M., Millan, R.M., Sample, J.G., Smith, D.M., Woodger, L.A., Masson, A., Narock, A.A., Asamura, K., Chang, T.F., Chiang, C.Y., Kazama, Y., Keika, K., Matsuda, S., Segawa, T., Seki, K., Shoji, M., Tam, S.W.Y., Umemura, N., Wang, B.J., Wang, S.Y., Redmon, R., Rodriguez, J.V., Singer, H.J., Vandegriff, J., Abe, S., Nose, M., Shinbori, A., Tanaka, Y.M., UeNo, S., Andersson, L., Dunn, P., Fowler, C., Halekas, J.S., Hara, T., Harada, Y., Lee, C.O., Lillis, R., Mitchell, D.L., Argall, M.R., Bromund, K., Burch, J.L., Cohen, I.J., Galloy, M., Giles, B., Jaynes, A.N., Le Contel, O., Oka, M., Phan, T.D., Walsh, B.M., Westlake, J., Wilder, F.D., Bale, S.D., Livi, R., Pulupa, M., Whittlesey, P., DeWolfe, A., Harter, B., Lucas, E., Auster, U., Bonnell, J.W., Cully, C.M., Donovan, E., Ergun, R.E., Frey, H.U., Jackel, B., Keiling, A., Korth, H., McFadden, J.P., Nishimura, Y., Plaschke, F., Robert, P., Turner, D.L., Weygand, J.M., Candey, R.M., Johnson, R.C., Kovalick, T., Liu, M.H., McGuire, R.E., Breneman, A., Kersten, K., Schroeder, P., 2019. The Space Physics Environment Data Analysis System (SPEDAS). *Space Sci. Rev.* 215, 9. 10.1007/s11214-018-0576-4.

- [13] Artemyev, A.V., Neishtadt, A.I., Albert, J.M., Gan, L., Li, W., Ma, Q., 2021a. Theoretical model of the nonlinear resonant interaction of whistler-mode waves and field-aligned electrons. *Physics of Plasmas* 28, 052902. 10.1063/5.0046635.
- [14] Artemyev, A.V., Neishtadt, A.I., Vainchtein, D.L., Vasiliev, A.A., Vasko, I.Y., Zelenyi, L.M., 2018a. Trapping (capture) into resonance and scattering on resonance: Summary of results for space plasma systems. *Communications in Nonlinear Science and Numerical Simulations* 65, 111–160. 10.1016/j.cnsns.2018.05.004.
- [15] Artemyev, A.V., Neishtadt, A.I., Vasiliev, A.A., 2020. Mapping for nonlinear electron interaction with whistler-mode waves. *Physics of Plasmas* 27, 042902. 10.1063/1.5144477, [arXiv:1911.11459](#).
- [16] Artemyev, A.V., Neishtadt, A.I., Vasiliev, A.A., Mourenas, D., 2017. Probabilistic approach to nonlinear wave-particle resonant interaction. *Phys. Rev. E* 95, 023204. 10.1103/PhysRevE.95.023204.
- [17] Artemyev, A.V., Neishtadt, A.I., Vasiliev, A.A., Mourenas, D., 2018b. Long-term evolution of electron distribution function due to nonlinear resonant interaction with whistler mode waves. *Journal of Plasma Physics* 84, 905840206. 10.1017/S0022377818000260.
- [18] Artemyev, A.V., Neishtadt, A.I., Vasiliev, A.A., Mourenas, D., 2021b. Transitional regime of electron resonant interaction with whistler-mode waves in inhomogeneous space plasma. *Phys. Rev. E* 104, 055203. 10.1103/PhysRevE.104.055203, [arXiv:2107.13511](#).
- [19] Artemyev, A.V., Shi, X., Liu, T.Z., Zhang, X.J., Vasko, I., Angelopoulos, V., 2022a. Electron Resonant Interaction With Whistler Waves Around Foreshock Transients and the Bow Shock Behind the Terminator. *Journal of Geophysical Research (Space Physics)* 127, e29820. 10.1029/2021JA029820.
- [20] Artemyev, A.V., Vasiliev, A.A., Mourenas, D., Neishtadt, A.I., Agapitov, O.V., Krasnosel'skikh, V., 2015. Probability of relativistic electron trapping by parallel and oblique whistler-mode waves in Earth's radiation belts. *Physics of Plasmas* 22, 112903. 10.1063/1.4935842.
- [21] Artemyev, A.V., Vasiliev, A.A., Neishtadt, A.I., 2019. Charged particle nonlinear resonance with localized electrostatic wave-packets. *Communications in Nonlinear Science and Numerical Simulations* 72, 392–406. 10.1016/j.cnsns.2019.01.011.
- [22] Artemyev, A.V., Zhang, X.J., Zou, Y., Mourenas, D., Angelopoulos, V., Vainchtein, D., Tsai, E., Wilkins, C., 2022b. On the Nature of Intense Sub-Relativistic Electron Precipitation. *Journal of Geophysical Research (Space Physics)* 127, e30571. 10.1029/2022JA030571.
- [23] Auster, H.U., Glassmeier, K.H., Magnes, W., Aydogar, O., Baumjohann, W., Constantinescu, D., Fischer, D., Fornacon, K.H., Georgescu, E., Harvey, P., Hillenmaier, O., Kroth, R., Ludlam, M., Narita, Y., Nakamura, R., Okrafka, K., Plaschke, F., Richter, I., Schwarzl, H., Stoll, B., Valavanoglou, A., Wiedemann, M., 2008. The THEMIS Fluxgate Magnetometer. *Space Sci. Rev.* 141, 235–264. 10.1007/s11214-008-9365-9.
- [24] Balikhin, M., Gedalin, M., Petrukovich, A., 1993. New mechanism for electron heating in shocks. *Physical Review Letters* 70, 1259–1262. 10.1103/PhysRevLett.70.1259.
- [25] Benkadda, S., Sen, A., Shklyar, D.R., 1996. Chaotic dynamics of charged particles in the field of two monochromatic waves in a magnetized plasma. *Chaos* 6, 451–460. 10.1063/1.166187.



- [26] Bohdan, A., 2023. Electron acceleration in supernova remnants. *Plasma Physics and Controlled Fusion* 65, 014002. [10.1088/1361-6587/aca5b2](https://doi.org/10.1088/1361-6587/aca5b2), [arXiv:2211.13992](https://arxiv.org/abs/2211.13992).
- [27] Bortnik, J., Thorne, R.M., Inan, U.S., 2008. Nonlinear interaction of energetic electrons with large amplitude chorus. *Geophys. Res. Lett.* 35, 21102. [10.1029/2008GL035500](https://doi.org/10.1029/2008GL035500).
- [28] Burgess, D., Scholer, M., 2013. Microphysics of Quasi-parallel Shocks in Collisionless Plasmas. *Space Sci. Rev.* 178, 513–533. [10.1007/s11214-013-9969-6](https://doi.org/10.1007/s11214-013-9969-6).
- [29] Cully, C.M., Ergun, R.E., Stevens, K., Nammari, A., Westfall, J., 2008. The THEMIS Digital Fields Board. *Space Sci. Rev.* 141, 343–355. [10.1007/s11214-008-9417-1](https://doi.org/10.1007/s11214-008-9417-1).
- [30] Demekhov, A.G., Trakhtengerts, V.Y., Rycroft, M.J., Nunn, D., 2006. Electron acceleration in the magnetosphere by whistler-mode waves of varying frequency. *Geomagnetism and Aeronomy* 46, 711–716. [10.1134/S0016793206060053](https://doi.org/10.1134/S0016793206060053).
- [31] Elkington, S.R., Chan, A.A., Jaynes, A.N., Malaspina, D., Albert, J., 2019. K2: Towards a Comprehensive Simulation Framework of the Van Allen Radiation Belts, in: *AGU Fall Meeting Abstracts*, pp. SM44B–01.
- [32] Elkington, S.R., Chan, A.A., Li, Z., Hudson, M.K., Jaynes, A.N., Baker, D.N., 2018. Generalizing Global Simulations of the Radiation Belts: Addressing Advective and Diffusive Processes in a Common Simulation Framework, in: *AGU Fall Meeting Abstracts*, pp. SM11B–02.
- [33] Frantsuzov, V.A., Artemyev, A.V., Zhang, X.J., Allanson, O., Shustov, P.I., Petrukovich, A.A., 2023. Diffusive scattering of energetic electrons by intense whistler-mode waves in an inhomogeneous plasma. *Journal of Plasma Physics* 89, 905890101. [10.1017/S0022377822001271](https://doi.org/10.1017/S0022377822001271).
- [34] Gan, L., Li, W., Ma, Q., Albert, J.M., Artemyev, A.V., Bortnik, J., 2020. Nonlinear Interactions Between Radiation Belt Electrons and Chorus Waves: Dependence on Wave Amplitude Modulation. *Geophys. Res. Lett.* 47, e85987. [10.1029/2019GL085987](https://doi.org/10.1029/2019GL085987).
- [35] Gan, L., Li, W., Ma, Q., Artemyev, A.V., Albert, J.M., 2022. Dependence of Nonlinear Effects on Whistler-Mode Wave Bandwidth and Amplitude: A Perspective From Diffusion Coefficients. *Journal of Geophysical Research (Space Physics)* 127, e30063. [10.1029/2021JA030063](https://doi.org/10.1029/2021JA030063).
- [36] Gedalin, M., 1996. Ion reflection at the shock front revisited. *J. Geophys. Res.* 101, 4871–4878. [10.1029/95JA03669](https://doi.org/10.1029/95JA03669).
- [37] Gedalin, M., 2020. Large-scale versus Small-scale Fields in the Shock Front: Effect on the Particle Motion. *Astrophys. J.* 895, 59. [10.3847/1538-4357/ab8af0](https://doi.org/10.3847/1538-4357/ab8af0).
- [38] Goodrich, C.C., Scudder, J.D., 1984. The adiabatic energy change of plasma electrons and the frame dependence of the cross-shock potential at collisionless magnetosonic shock waves. *J. Geophys. Res.* 89, 6654–6662. [10.1029/JA089iA08p06654](https://doi.org/10.1029/JA089iA08p06654).
- [39] Hiraga, R., Omura, Y., 2020. Acceleration mechanism of radiation belt electrons through interaction with multi-subpacket chorus waves. *Earth, Planets, and Space* 72, 21. [10.1186/s40623-020-1134-3](https://doi.org/10.1186/s40623-020-1134-3).
- [40] Hsieh, Y.K., Kubota, Y., Omura, Y., 2020. Nonlinear Evolution of Radiation Belt Electron Fluxes Interacting With Oblique Whistler Mode Chorus Emissions. *Journal of Geophysical Research (Space Physics)* 125, e27465. [10.1029/2019JA027465](https://doi.org/10.1029/2019JA027465).

- [41] Hsieh, Y.K., Omura, Y., 2017. Nonlinear dynamics of electrons interacting with oblique whistler mode chorus in the magnetosphere. *J. Geophys. Res.* 122, 675–694. 10.1002/2016JA023255.
- [42] Hull, A.J., Chaston, C.C., Bonnell, J.W., Damiano, P.A., Wygant, J.R., Reeves, G.D., 2020. Correlations Between Dispersive Alfvén Wave Activity, Electron Energization, and Ion Outflow in the Inner Magnetosphere. *Geophys. Res. Lett.* 47, e88985. 10.1029/2020GL088985.
- [43] Hull, A.J., Muschietti, L., Oka, M., Larson, D.E., Mozer, F.S., Chaston, C.C., Bonnell, J.W., Hospodarsky, G.B., 2012. Multiscale whistler waves within Earth’s perpendicular bow shock. *J. Geophys. Res.* 117, 12104. 10.1029/2012JA017870.
- [44] Karpman, V.I., 1974. Nonlinear Effects in the ELF Waves Propagating along the Magnetic Field in the Magnetosphere. *Space Sci. Rev.* 16, 361–388. 10.1007/BF00171564.
- [45] Karpman, V.I., Istomin, I.N., Shkliar, D.R., 1975. Effects of nonlinear interaction of monochromatic waves with resonant particles in the inhomogeneous plasma. *Physica Scripta* 11, 278–284. 10.1088/0031-8949/11/5/008.
- [46] Khazanov, G.V., Tel’nikhin, A.A., Kronberg, T.K., 2013. Radiation belt electron dynamics driven by large-amplitude whistlers. *Journal of Geophysical Research (Space Physics)* 118, 6397–6404. 10.1002/2013JA019122.
- [47] Khazanov, G.V., Tel’nikhin, A.A., Kronberg, T.K., 2014. Stochastic electron motion driven by space plasma waves. *Nonlinear Processes in Geophysics* 21, 61–85. 10.5194/npg-21-61-2014.
- [48] Kitahara, M., Katoh, Y., 2019. Anomalous Trapping of Low Pitch Angle Electrons by Coherent Whistler Mode Waves. *J. Geophys. Res.* 124, 5568–5583. 10.1029/2019JA026493.
- [49] Krasnoselskikh, V., Balikhin, M., Walker, S.N., Schwartz, S., Sundkvist, D., Lobzin, V., Gedalin, M., Bale, S.D., Mozer, F., Soucek, J., Hobara, Y., Comisel, H., 2013. The Dynamic Quasiperpendicular Shock: Cluster Discoveries. *Space Sci. Rev.* 178, 535–598. 10.1007/s11214-013-9972-y, arXiv:1303.0190.
- [50] Kuramitsu, Y., Krasnoselskikh, V., 2005. Gyroresonant Surfing Acceleration. *Physical Review Letters* 94, 031102–+. 10.1103/PhysRevLett.94.031102.
- [51] Le Contel, O., Roux, A., Robert, P., Coillot, C., Bouabdellah, A., de La Porte, B., Alison, D., Ruocco, S., Angelopoulos, V., Bromund, K., Chaston, C.C., Cully, C., Auster, H.U., Glassmeier, K.H., Baumjohann, W., Carlson, C.W., McFadden, J.P., Larson, D., 2008. First Results of the THEMIS Search Coil Magnetometers. *Space Sci. Rev.* 141, 509–534. 10.1007/s11214-008-9371-y.
- [52] Le Queau, D., Roux, A., 1987. Quasi-monochromatic wave-particle interactions in magnetospheric plasmas. *Solar Physics* 111, 59–80. 10.1007/BF00145441.
- [53] Leroy, M.M., Mangeney, A., 1984. A theory of energization of solar wind electrons by the earth’s bow shock. *Annales Geophysicae* 2, 449–456.
- [54] Lichko, E., Egedal, J., 2020. Magnetic pumping model for energizing superthermal particles applied to observations of the Earth’s bow shock. *Nature Communications* 11, 2942. 10.1038/s41467-020-16660-4.

- [55] Lin, Y., 1997. Generation of anomalous flows near the bow shock by its interaction with interplanetary discontinuities. *J. Geophys. Res.* 102, 24265–24282. 10.1029/97JA01989.
- [56] Lin, Y., 2002. Global hybrid simulation of hot flow anomalies near the bow shock and in the magnetosheath. *Plan. Sp. Sci.* 50, 577–591. 10.1016/S0032-0633(02)00037-5.
- [57] Lin, Y., Wang, X.Y., Lu, S., Perez, J.D., Lu, Q., 2014. Investigation of storm time magnetotail and ion injection using three-dimensional global hybrid simulation. *J. Geophys. Res.* 119, 7413–7432. 10.1002/2014JA020005.
- [58] Liu, T.Z., Angelopoulos, V., Lu, S., 2019. Relativistic electrons generated at Earth’s quasi-parallel bow shock. *Science Advances* 5, eaaw1368. 10.1126/sciadv.aaw1368.
- [59] Liu, T.Z., Lu, S., Angelopoulos, V., Hietala, H., Wilson, L.B., 2017. Fermi acceleration of electrons inside foreshock transient cores. *Journal of Geophysical Research (Space Physics)* 122, 9248–9263. 10.1002/2017JA024480, arXiv:1706.05047.
- [60] Liu, T.Z., Turner, D.L., Angelopoulos, V., Omid, N., 2016. Multipoint observations of the structure and evolution of foreshock bubbles and their relation to hot flow anomalies. *Journal of Geophysical Research* 121, 5489–5509. 10.1002/2016JA022461.
- [61] Lukin, A.S., Artemyev, A.V., Petrukovich, A.A., 2021. On application of stochastic differential equations for simulation of nonlinear wave-particle resonant interactions. *Physics of Plasmas* 28, 092904. 10.1063/5.0058054, arXiv:2105.05819.
- [62] Lundin, B.V., Shkliar, D.R., 1977. Interaction of electrons with low transverse velocities with VLF waves in an inhomogeneous plasma. *Geomagnetism and Aeronomy* 17, 246–251.
- [63] Lyons, L.R., Williams, D.J., 1984. Quantitative aspects of magnetospheric physics.
- [64] McFadden, J.P., Carlson, C.W., Larson, D., Ludlam, M., Abiad, R., Elliott, B., Turin, P., Marckwordt, M., Angelopoulos, V., 2008. The THEMIS ESA Plasma Instrument and In-flight Calibration. *Space Sci. Rev.* 141, 277–302. 10.1007/s11214-008-9440-2.
- [65] Mitchell, J.J., Schwartz, S.J., 2013. Nonlocal electron heating at the Earth’s bow shock and the role of the magnetically tangent point. *Journal of Geophysical Research (Space Physics)* 118, 7566–7575. 10.1002/2013JA019226.
- [66] Mitchell, J.J., Schwartz, S.J., 2014. Isothermal magnetosheath electrons due to nonlocal electron cross talk. *Journal of Geophysical Research (Space Physics)* 119, 1080–1093. 10.1002/2013JA019211.
- [67] Morris, P.J., Bohdan, A., Weidl, M.S., Tsiros, M., Fulat, K., Pohl, M., 2023. Pre-acceleration in the Electron Foreshock II: Oblique Whistler Waves. arXiv e-prints, arXiv:2301.00872 arXiv:2301.00872.
- [68] Mourenas, D., Zhang, X.J., Artemyev, A.V., Angelopoulos, V., Thorne, R.M., Bortnik, J., Neishtadt, A.I., Vasiliev, A.A., 2018. Electron Nonlinear Resonant Interaction With Short and Intense Parallel Chorus Wave Packets. *J. Geophys. Res.* 123, 4979–4999. 10.1029/2018JA025417.

- [69] Mourenas, D., Zhang, X.J., Nunn, D., Artemyev, A.V., Angelopoulos, V., Tsai, E., Wilkins, C., 2022. Short Chorus Wave Packets: Generation Within Chorus Elements, Statistics, and Consequences on Energetic Electron Precipitation. *Journal of Geophysical Research (Space Physics)* 127, e30310. [10.1029/2022JA030310](https://doi.org/10.1029/2022JA030310).
- [70] Nunn, D., 1986. A nonlinear theory of sideband stability in ducted whistler mode waves. *Plan. Sp. Sci.* 34, 429–451. [10.1016/0032-0633\(86\)90032-2](https://doi.org/10.1016/0032-0633(86)90032-2).
- [71] Nunn, D., Zhang, X.J., Mourenas, D., Artemyev, A.V., 2021. Generation of Realistic Short Chorus Wave Packets. *Geophys. Res. Lett.* 48, e92178. [10.1029/2020GL092178](https://doi.org/10.1029/2020GL092178).
- [72] Oka, M., Otsuka, F., Matsukiyo, S., Wilson, L. B., I., Argall, M.R., Amano, T., Phan, T.D., Hoshino, M., Le Contel, O., Gershman, D.J., Burch, J.L., Torbert, R.B., Dorelli, J.C., Giles, B.L., Ergun, R.E., Russell, C.T., Lindqvist, P.A., 2019. Electron Scattering by Low-frequency Whistler Waves at Earth’s Bow Shock. *Astrophys. J.* 886, 53. [10.3847/1538-4357/ab4a81](https://doi.org/10.3847/1538-4357/ab4a81).
- [73] Oka, M., Wilson, III, L.B., Phan, T.D., Hull, A.J., Amano, T., Hoshino, M., Argall, M.R., Le Contel, O., Agapitov, O., Gershman, D.J., Khotyaintsev, Y.V., Burch, J.L., Torbert, R.B., Pollock, C., Dorelli, J.C., Giles, B.L., Moore, T.E., Saito, Y., Avakov, L.A., Paterson, W., Ergun, R.E., Strangeway, R.J., Russell, C.T., Lindqvist, P.A., 2017. Electron Scattering by High-frequency Whistler Waves at Earth’s Bow Shock. *Astrophys. J. Lett.* 842, L11. [10.3847/2041-8213/aa7759](https://doi.org/10.3847/2041-8213/aa7759).
- [74] Omelchenko, Y.A., Roytershteyn, V., Chen, L.J., Ng, J., Hietala, H., 2021. HYPERS simulations of solar wind interactions with the Earth’s magnetosphere and the Moon. *Journal of Atmospheric and Solar-Terrestrial Physics* 215, 105581. [10.1016/j.jastp.2021.105581](https://doi.org/10.1016/j.jastp.2021.105581).
- [75] Omid, N., Berchem, J., Sibeck, D., Zhang, H., 2016. Impacts of spontaneous hot flow anomalies on the magnetosheath and magnetopause. *Journal of Geophysical Research (Space Physics)* 121, 3155–3169. [10.1002/2015JA022170](https://doi.org/10.1002/2015JA022170).
- [76] Omid, N., Sibeck, D.G., 2007. Formation of hot flow anomalies and solitary shocks. *Journal of Geophysical Research (Space Physics)* 112, A01203. [10.1029/2006JA011663](https://doi.org/10.1029/2006JA011663).
- [77] Omid, N., Sibeck, D.G., Blanco-Cano, X., 2009. Foreshock compressional boundary. *Journal of Geophysical Research (Space Physics)* 114, A08205. [10.1029/2008JA013950](https://doi.org/10.1029/2008JA013950).
- [78] Omura, Y., Furuya, N., Summers, D., 2007. Relativistic turning acceleration of resonant electrons by coherent whistler mode waves in a dipole magnetic field. *J. Geophys. Res.* 112, 6236. [10.1029/2006JA012243](https://doi.org/10.1029/2006JA012243).
- [79] Omura, Y., Matsumoto, H., Nunn, D., Rycroft, M.J., 1991. A review of observational, theoretical and numerical studies of VLF triggered emissions. *Journal of Atmospheric and Terrestrial Physics* 53, 351–368.
- [80] Omura, Y., Miyashita, Y., Yoshikawa, M., Summers, D., Hikishima, M., Ebihara, Y., Kubota, Y., 2015. Formation process of relativistic electron flux through interaction with chorus emissions in the Earth’s inner magnetosphere. *J. Geophys. Res.* 120, 9545–9562. [10.1002/2015JA021563](https://doi.org/10.1002/2015JA021563).
- [81] Page, B., Vasko, I.Y., Artemyev, A.V., Bale, S.D., 2021. Generation of High-frequency Whistler Waves in the Earth’s Quasi-perpendicular Bow Shock. *Astrophys. J. Lett.* 919, L17. [10.3847/2041-8213/ac2748](https://doi.org/10.3847/2041-8213/ac2748).

- [82] Schulz, M., Lanzerotti, L.J., 1974. Particle diffusion in the radiation belts. Springer, New York.
- [83] Scudder, J.D., 1995. A review of the physics of electron heating at collisionless shocks. *Advances in Space Research* 15, 181–223. [10.1016/0273-1177\(94\)00101-6](https://doi.org/10.1016/0273-1177(94)00101-6).
- [84] See, V., Cameron, R.F., Schwartz, S.J., 2013. Non-adiabatic electron behaviour due to short-scale electric field structures at collisionless shock waves. *Annales Geophysicae* 31, 639–646. [10.5194/angeo-31-639-2013](https://doi.org/10.5194/angeo-31-639-2013), [arXiv:1304.4841](https://arxiv.org/abs/1304.4841).
- [85] Shapiro, V.D., Sagdeev, R.Z., 1997. Nonlinear wave-particle interaction and conditions for the applicability of quasilinear theory. *Physics Reports* 283, 49–71. [10.1016/S0370-1573\(96\)00053-1](https://doi.org/10.1016/S0370-1573(96)00053-1).
- [86] Shi, X., Liu, T., Artemyev, A., Angelopoulos, V., Zhang, X.J., Turner, D.L., 2023. Intense Whistler-mode Waves at Foreshock Transients: Characteristics and Regimes of Wave-Particle Resonant Interaction. *Astrophys. J.* 944, 193. [10.3847/1538-4357/acb543](https://doi.org/10.3847/1538-4357/acb543), [arXiv:2211.05398](https://arxiv.org/abs/2211.05398).
- [87] Shi, X., Liu, T.Z., Angelopoulos, V., Zhang, X.J., 2020. Whistler Mode Waves in the Compressional Boundary of Foreshock Transients. *Journal of Geophysical Research (Space Physics)* 125, e27758. [10.1029/2019JA027758](https://doi.org/10.1029/2019JA027758).
- [88] Shklyar, D.R., 2021. A Theory of Interaction Between Relativistic Electrons and Magnetically Reflected Whistlers. *Journal of Geophysical Research (Space Physics)* 126, e28799. [10.1029/2020JA028799](https://doi.org/10.1029/2020JA028799).
- [89] Shklyar, D.R., Matsumoto, H., 2009. Oblique Whistler-Mode Waves in the Inhomogeneous Magnetospheric Plasma: Resonant Interactions with Energetic Charged Particles. *Surveys in Geophysics* 30, 55–104. [10.1007/s10712-009-9061-7](https://doi.org/10.1007/s10712-009-9061-7).
- [90] Stix, T.H., 1962. *The Theory of Plasma Waves*.
- [91] Tao, X., Bortnik, J., Albert, J.M., Thorne, R.M., Li, W., 2013. The importance of amplitude modulation in nonlinear interactions between electrons and large amplitude whistler waves. *Journal of Atmospheric and Solar-Terrestrial Physics* 99, 67–72. [10.1016/j.jastp.2012.05.012](https://doi.org/10.1016/j.jastp.2012.05.012).
- [92] Tao, X., Chan, A.A., Albert, J.M., Miller, J.A., 2008. Stochastic modeling of multidimensional diffusion in the radiation belts. *Journal of Geophysical Research (Space Physics)* 113, A07212. [10.1029/2007JA012985](https://doi.org/10.1029/2007JA012985).
- [93] Tong, Y., Vasko, I.Y., Artemyev, A.V., Bale, S.D., Mozer, F.S., 2019. Statistical Study of Whistler Waves in the Solar Wind at 1 au. *Astrophys. J.* 878, 41. [10.3847/1538-4357/ab1f05](https://doi.org/10.3847/1538-4357/ab1f05), [arXiv:1905.08958](https://arxiv.org/abs/1905.08958).
- [94] Trakhtengerts, V.Y., Rycroft, M.J., Nunn, D., Demekhov, A.G., 2003. Cyclotron acceleration of radiation belt electrons by whistlers. *J. Geophys. Res.* 108, 1138. [10.1029/2002JA009559](https://doi.org/10.1029/2002JA009559).
- [95] Tsai, E., Artemyev, A., Zhang, X.J., Angelopoulos, V., 2022. Relativistic Electron Precipitation Driven by Nonlinear Resonance With Whistler-Mode Waves. *Journal of Geophysical Research (Space Physics)* 127, e30338. [10.1029/2022JA030338](https://doi.org/10.1029/2022JA030338).

- [96] Turner, D.L., Omid, N., Sibeck, D.G., Angelopoulos, V., 2013. First observations of foreshock bubbles upstream of Earth's bow shock: Characteristics and comparisons to HFAs. *Journal of Geophysical Research (Space Physics)* 118, 1552–1570. [10.1002/jgra.50198](https://doi.org/10.1002/jgra.50198).
- [97] Vainchtein, D., Zhang, X.J., Artemyev, A.V., Mourenas, D., Angelopoulos, V., Thorne, R.M., 2018. Evolution of Electron Distribution Driven by Nonlinear Resonances With Intense Field-Aligned Chorus Waves. *Journal of Geophysical Research (Space Physics)* 123, 8149–8169. [10.1029/2018JA025654](https://doi.org/10.1029/2018JA025654), [arXiv:1806.00066](https://arxiv.org/abs/1806.00066).
- [98] Vasko, I.Y., Kuzichev, I.V., Artemyev, A.V., Bale, S.D., Bonnell, J.W., Mozer, F.S., 2020. On quasi-parallel whistler waves in the solar wind. *Physics of Plasmas* 27, 082902. [10.1063/5.0003401](https://doi.org/10.1063/5.0003401), [arXiv:2005.12606](https://arxiv.org/abs/2005.12606).
- [99] Veltri, P., Zimbardo, G., 1993a. Electron-whistler interaction at the Earth's bow shock: 1. Whistler instability. *J. Geophys. Res.* 98, 13325–13334. [10.1029/93JA00812](https://doi.org/10.1029/93JA00812).
- [100] Veltri, P., Zimbardo, G., 1993b. Electron-whistler interaction at the Earth's bow shock: 2. Electron pitch angle diffusion. *J. Geophys. Res.* 98, 13335–13346. [10.1029/93JA01144](https://doi.org/10.1029/93JA01144).
- [101] von Alfthan, S., Pokhotelov, D., Kempf, Y., Hoilijoki, S., Honkonen, I., Sandroos, A., Palmroth, M., 2014. Vlasiator: First global hybrid-Vlasov simulations of Earth's foreshock and magnetosheath. *Journal of Atmospheric and Solar-Terrestrial Physics* 120, 24–35. [10.1016/j.jastp.2014.08.012](https://doi.org/10.1016/j.jastp.2014.08.012).
- [102] Wilson, L.B., 2016. Low Frequency Waves at and Upstream of Collisionless Shocks. Washington DC American Geophysical Union Geophysical Monograph Series 216, 269–291. [10.1002/9781119055006.ch16](https://doi.org/10.1002/9781119055006.ch16).
- [103] Wilson, L.B., Koval, A., Szabo, A., Breneman, A., Cattell, C.A., Goetz, K., Kellogg, P.J., Kersten, K., Kasper, J.C., Maruca, B.A., Pulupa, M., 2013. Electromagnetic waves and electron anisotropies downstream of supercritical interplanetary shocks. *J. Geophys. Res.* 118, 5–16. [10.1029/2012JA018167](https://doi.org/10.1029/2012JA018167), [arXiv:1207.6429](https://arxiv.org/abs/1207.6429).
- [104] Wilson, L.B., Sibeck, D.G., Turner, D.L., Osmane, A., Caprioli, D., Angelopoulos, V., 2016. Relativistic Electrons Produced by Foreshock Disturbances Observed Upstream of Earth's Bow Shock. *Physical Review Letters* 117, 215101. [10.1103/PhysRevLett.117.215101](https://doi.org/10.1103/PhysRevLett.117.215101), [arXiv:1607.02183](https://arxiv.org/abs/1607.02183).
- [105] Wilson, III, L.B., Koval, A., Szabo, A., Breneman, A., Cattell, C.A., Goetz, K., Kellogg, P.J., Kersten, K., Kasper, J.C., Maruca, B.A., Pulupa, M., 2012. Observations of electromagnetic whistler precursors at supercritical interplanetary shocks. *Geophys. Res. Lett.* 39, 8109. [10.1029/2012GL051581](https://doi.org/10.1029/2012GL051581).
- [106] Wilson, III, L.B., Stevens, M.L., Kasper, J.C., Klein, K.G., Maruca, B.A., Bale, S.D., Bowen, T.A., Pulupa, M.P., Salem, C.S., 2018. The Statistical Properties of Solar Wind Temperature Parameters Near 1 au. *Astrophys. J. Supplement Series* 236, 41. [10.3847/1538-4365/aab71c](https://doi.org/10.3847/1538-4365/aab71c), [arXiv:1802.08585](https://arxiv.org/abs/1802.08585).
- [107] Wu, C.S., 1984. A fast Fermi process: Energetic electrons accelerated by a nearly perpendicular bow shock. *J. Geophys. Res.* 89, 8857–8862. [10.1029/JA089iA10p08857](https://doi.org/10.1029/JA089iA10p08857).

- [108] Zhang, H., Zong, Q., Connor, H., Delamere, P., Facskó, G., Han, D., Hasegawa, H., Kallio, E., Kis, Á., Le, G., Lembège, B., Lin, Y., Liu, T., Oksavik, K., Omid, N., Otto, A., Ren, J., Shi, Q., Sibeck, D., Yao, S., 2022. Dayside Transient Phenomena and Their Impact on the Magnetosphere and Ionosphere. *Space Sci. Rev.* 218, 40. [10.1007/s11214-021-00865-0](https://doi.org/10.1007/s11214-021-00865-0).
- [109] Zhang, X.J., Agapitov, O., Artemyev, A.V., Mourenas, D., Angelopoulos, V., Kurth, W.S., Bonnell, J.W., Hospodarsky, G.B., 2020. Phase Decoherence Within Intense Chorus Wave Packets Constrains the Efficiency of Nonlinear Resonant Electron Acceleration. *Geophys. Res. Lett.* 47, e89807. [10.1029/2020GL089807](https://doi.org/10.1029/2020GL089807).
- [110] Zhang, X.J., Thorne, R., Artemyev, A., Mourenas, D., Angelopoulos, V., Bortnik, J., Kletzing, C.A., Kurth, W.S., Hospodarsky, G.B., 2018. Properties of Intense Field-Aligned Lower-Band Chorus Waves: Implications for Nonlinear Wave-Particle Interactions. *Journal of Geophysical Research (Space Physics)* 123, 5379–5393. [10.1029/2018JA025390](https://doi.org/10.1029/2018JA025390).